

Phonon-assisted damping of plasmons in three- and two-dimensional metals

Fabio Caruso,¹ Dino Novko,² and Claudia Draxl¹

¹*Institut für Physik and IRIS Adlershof, Humboldt-Universität zu Berlin, Berlin, Germany*

²*Institut für Chemie und Biochemie, Freie Universität Berlin, Takustr. 3, 14195 Berlin, Germany*

(Dated: March 15, 2022)

We investigate the effects of crystal lattice vibrations on the dispersion of plasmons. The loss function of the homogeneous electron gas (HEG) in two and three dimensions is evaluated numerically in presence of electronic coupling to an optical phonon mode. Our calculations are based on many-body perturbation theory for the dielectric function as formulated by the Hedin-Baym equations in the Fan-Migdal approximation. The coupling to phonons broadens the spectral signatures of plasmons in the electron-energy loss spectrum (EELS) and it induces the decay of plasmons on timescales shorter than 1 ps. Our results further reveal the formation of a kink in the plasmon dispersion of the 2D HEG, which marks the onset of plasmon-phonon scattering. Overall, these features constitute a fingerprint of plasmon-phonon coupling in the EELS of simple metals. It is shown that these effects may be accounted for by resorting to a simplified treatment of the electron-phonon interaction which is amenable to first-principles calculations.

I. INTRODUCTION

The coupling between electrons and crystal lattice vibrations (phonons) affects pervasively the quantum behaviour of condensed matter.¹ It underpins a broad spectrum of emergent phenomena, including kinks and polaronic satellites in photoemission,^{2–6} the temperature dependence of electronic bands,^{7–12} and optical spectra,^{13–15} (non-adiabatic) Kohn anomalies,^{16–19} and conventional superconductivity.²⁰ Electron-phonon scattering also constitutes one of the primary decay channels that drives dissipation phenomena in solids such as, e.g., hot carrier relaxation,^{21–23} the decay of collective charge-density fluctuations (plasmons),^{24–26} and phonon damping.²⁷ A quantitative understanding of these mechanisms through first-principles simulations may open new ways towards the identification of materials for applications where the characteristic time-scales of the dissipation processes are critical for the device function.

Plasmonics, for instance, employs plasmons and surface plasmon polaritons (SPP) to manipulate light-matter interactions at the nano-scale, and it has proven successful in an interdisciplinary area of applications, encompassing, e.g., photovoltaics,²⁸ radiation therapy,^{29,30} and sensing.³¹ Since long plasmon lifetimes precondition the functionality of plasmonic devices,³² dissipation mechanisms arising from electron-electron and electron-lattice scattering, which are at the origin of plasmon damping (the decay of plasmons and SPP), presently constitute a major bottleneck for plasmonics. The development of predictive theories and simulation tools for the study of phonon-assisted dissipation may provide a new impulse to unravel the origin of plasmon damping and address the issue of quantum losses in plasmonics.

A plasmon is excited at momenta \mathbf{q} and frequencies ω_{pl} which correspond to zeros of the macroscopic dielectric function.³³ A fully quantum-mechanical description of phonon-assisted plasmon damping, where a plasmon annihilates through the emission of a phonon, requires to account for the interplay between plasmons and phonons

by generalizing the dielectric function to the coupled electron-phonon system.³⁴ Recent years have witnessed remarkable advancements along this line. The temperature dependence of the absorption onset of indirect band-gap semiconductors, a phenomenon dominated by phonon-assisted processes, has motivated the formulation of a theory of optical absorption based on Fermi's golden rule,³⁵ as well as a generalization of William-Lax theory for phonon-assisted optical absorption to first-principles calculations^{36,37} and its extension to non-stochastic one-shot calculations.³⁸ An alternative procedure to account for the coupling to phonons in the evaluation of the dielectric function consists in introducing quasiparticle effects due to electron-phonon interaction in the Bethe-Salpeter equation, a procedure that has been applied to silicon¹⁵ and to transition metal dichalcogenides,³⁹ and through the formulation of a many-body theory of exciton-phonon interaction.⁴⁰ While these works have primarily addressed the temperature dependence of absorption spectroscopy experiments, only recently the effects of electron-phonon coupling on the damping of plasmons have been accounted for from first principles.²⁶

In this manuscript, we introduce a field-theoretic formalism which, based on the Hedin-Baym equations, a formally exact formulation of the problems of interacting electrons and phonons in the harmonic approximation, allows the investigation of the damping of plasmons induced by the electron-phonon interaction. Numerical results for the plasmon dispersion of the homogeneous electron gas (HEG) are reported in two (2D) and three dimensions (3D) at carrier densities representative of metals and highly-doped semiconductors. Plasmon-damping effects arising from electronic coupling to a non-dispersive optical phonon are investigated through the computation of the loss function. In 3D, the electron-phonon interaction introduces finite-lifetime effects that significantly broaden the plasmon dispersion, providing a fingerprint of phonon-assisted plasmon damping in 3D metals. In 2D metallic systems, the proximity of the phonon and plasmon energies at long wavelengths gives

rise to a kink in the plasmon dispersion. This novel spectroscopic signature of plasmon-phonon coupling, reminiscent of the photoemission kinks of superconductors⁴³ and pristine graphene,⁴⁴ manifests itself at the energy and momentum that mark the onset of plasmon-phonon scattering. The accuracy of approximate techniques to account for plasmon-phonon interaction in first-principles calculations at a reduced computational cost is further discussed. Beside providing a many-body formalism for the description of phonon-assisted plasmon damping, this study contributes to unveil novel spectral signatures resulting from plasmon-phonon coupling, a result that may prove useful for the characterization of plasmonic materials with reduced dimensionality such as, e.g., doped graphene or single-layer transition metal dichalcogenides.

The manuscript is organized as follows. In Sec. II we report the Hedin-Baym equations for the dielectric function and the procedure followed for their solution in the Fan-Migdal approximation. Numerical results for the 3D HEG are presented in Sec. III, whereas Sec. IV illustrates the two-dimensional case. In Sec. V the accuracy of approximate procedures to account for electron-phonon coupling effects in the evaluation of the dielectric function are discussed. Finally, concluding remarks are presented in Sec. VI.

II. HEDIN-BAYM EQUATIONS FOR THE DIELECTRIC FUNCTION

Many-body perturbation theory provides a suitable framework to investigate the effects of the electron-phonon interaction on the plasmon dispersions of metals. Hedin's equations for the single-particle Green function constitute an exact formulation of the many-body problem under the assumption that the nuclei are fixed at their equilibrium position (*clamped-nuclei approximation*).⁴¹ Hedin's equations can be generalized to account for the coupling between nuclear and electronic degrees of freedom by explicitly considering the variation of the total electronic potential up to the second order in the atomic displacement (harmonic approximation). The resulting set of equations, denoted as the Hedin-Baym equations, constitute a formally exact framework for describing a electron-phonon system within the harmonic approximation.¹ Within this formalism, the dielectric function is determined by the following set of equations:

$$\varepsilon(12) = \delta(12) - \int d(3)v(13)P(32)$$

$$P(12) = -i \int d(34)G(13)G(41^+)\Gamma(342)$$

$$G(12) = G_0(12) + \int d(34)G_0(13)\Sigma(34)G(42)$$

$$\Sigma(12) = i\hbar \int d(34)G(13)\Gamma(342)[W_e(41^+) + W_{\text{ph}}(41^+)]$$

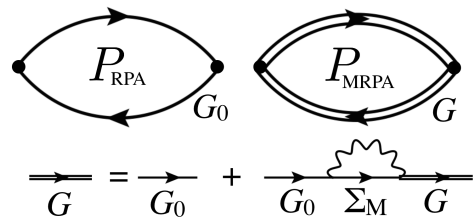


Figure 1. Feynman diagrams for the irreducible polarization: Left: RPA, right: polarizability obtained through the inclusion of electron-phonon coupling effects at first-order within the Fan-Migdal approximation (MRPA).

Here the collective index $1 \equiv \mathbf{r}_1, t_1$ has been introduced. ε is the dielectric function, P the irreducible electronic polarization, Σ the electron self-energy due to the combined effects of electrons and phonons, G and G_0 the interacting and non-interacting Green functions, and Γ the three-point vertex function. v denotes the bare Coulomb interaction, whereas W_e and W_{ph} are the screened Coulomb interactions due to electron-electron and electron-phonon interaction, respectively, which are related by the expression¹ (in symbolic notation) $W_{\text{ph}} = W_e D W_e$, with D being the phonon Green function.

Analogously to the *GW* method,^{41,46} the Hedin-Baym equations should be solved self-consistently⁴⁷⁻⁴⁹ owing to the interdependence of polarization, Green function, and self-energy. In the following, to define a practical procedure for the computational evaluation of the dielectric function, we restrict ourselves to consider one-shot calculations of the polarizability and dielectric function, where the Green function is obtained from a single solution of the Dyson equation. Additionally, we set the vertex function to $\Gamma(123) = \delta(13)\delta(23)$, which corresponds to the Fan-Migdal approximation for the self-energy. In practice, this approximation consists in ignoring the contribution of electron-phonon coupling on the interaction between electrons and holes. We concentrate on the electron-phonon interaction, and thus ignore the effects of the electron-electron interaction beyond the single-particle picture by neglecting the electronic part of the screened interaction W_e in the self-energy Σ . Within these approximations, and considering the Fourier transform of the Hedin-Baym equations to momentum and frequency, the defining equation for the dielectric function of the coupled electron-phonon system may be rewritten as:

$$\varepsilon(\mathbf{q}, \omega) = 1 - v(\mathbf{q})P(\mathbf{q}, \omega) \quad (1)$$

$$P(\mathbf{q}, \omega) = i \int \frac{d\mathbf{k} d\omega'}{(2\pi)^4} G(\mathbf{q} + \mathbf{k}, \omega + \omega') G(\mathbf{k}, \omega') \quad (2)$$

$$G(\mathbf{k}, \omega) = [\hbar\omega - \epsilon_{\mathbf{k}} - \Sigma_{\text{M}}(\mathbf{k}, \omega)]^{-1} \quad (3)$$

$$\Sigma_{\text{M}}(\mathbf{k}, \omega) = \frac{i}{\hbar} \sum_{\nu} \int \frac{d\mathbf{q} d\omega'}{(2\pi)^4} |g_{\mathbf{k}\mathbf{q}}^{\nu}|^2 \times G_0(\mathbf{q} + \mathbf{k}, \omega + \omega') D_0^{\nu}(\mathbf{q}, \omega') \quad (4)$$

where $\epsilon_{\mathbf{k}}$ are the single-particle energies of non-interacting electrons, $g_{\mathbf{k}\mathbf{q}}^{\nu}$ the electron-phonon coupling matrix elements, ν and $\hbar\omega_{\mathbf{q}\nu}$ the phonon-mode index and energy, and $D_0^{\nu}(\mathbf{q}, \omega) = 2\omega_{\mathbf{q}\nu}[\omega^2 - \omega_{\mathbf{q}\nu}^2]^{-1}$ the non-interacting Green function for the ν -th phonon. Σ_M is the Fan-Migdal electron self-energy due to electron-phonon interaction, and it is derived following standard field-theoretic approaches.¹ The procedure defined by Eqs. (1)-(4) extends the random-phase approximation (RPA) for the irreducible polarization P to the interacting electron-phonon system by replacing the non-interacting Green function with a propagator *dressed* by the electron-phonon interaction in the Fan-Migdal approximation. A Feynman-diagrammatic representation of the polarizability in this approximation is compared to the RPA in Fig. 1. If the Fan-Migdal self-energy is set to zero, G reduces to the non-interacting Green function G_0 and P to the RPA.

One may promptly verify that the combination of the Dyson equation with Eq. (2) yields the following expression for the polarizability:⁵⁰

$$P(\mathbf{q}, \omega) = i \sum_{\mathbf{k}\sigma} \int \frac{d\omega'}{2\pi} \frac{G(\mathbf{k}, \omega') - G(\mathbf{k} + \mathbf{q}, \omega + \omega')}{\hbar\omega + \epsilon_{\mathbf{k}} - \epsilon_{\mathbf{k}+\mathbf{q}} + \Delta\Sigma(\mathbf{k}, \mathbf{q}, \omega, \omega')}$$

where the quantity $\Delta\Sigma(\mathbf{k}, \mathbf{q}, \omega, \omega') = \Sigma_M(\mathbf{k}, \omega') - \Sigma_M(\mathbf{k} + \mathbf{q}, \omega + \omega')$, sometimes denoted as electron-hole self-energy⁵⁰ or optical self-energy,⁵¹ has been introduced. The polarizability can thus be rewritten as:^{34,50}

$$P(\mathbf{q}, \omega) = 2 \sum_{\mathbf{k}} \frac{f_{\mathbf{k}} - f_{\mathbf{k}+\mathbf{q}}}{\hbar\omega + \epsilon_{\mathbf{k}} - \epsilon_{\mathbf{k}+\mathbf{q}} + \Delta\Sigma(\mathbf{k}, \mathbf{q}, \omega, \epsilon_{\mathbf{k}}/\hbar)}. \quad (5)$$

Equation (5) is obtained by neglecting the ω' dependence of the electron-hole self-energy and performing the frequency integration only in the numerator, which yield the Fermi-Dirac occupation factors $f_{\mathbf{k}}$. The combination of Eqs. (1) and (5) provides a practical recipe for incorporating the effects of electron-phonon coupling in the dielectric function. Inspection of Eq. (5) suggests that the interaction with phonons in the Fan-Migdal approximation may be approximately accounted for by replacing $\epsilon_{\mathbf{k}} \rightarrow \epsilon_{\mathbf{k}} + \Sigma_M(\mathbf{k}, \epsilon_{\mathbf{k}}/\hbar)$ and $\epsilon_{\mathbf{k}+\mathbf{q}} \rightarrow \epsilon_{\mathbf{k}+\mathbf{q}} + \Sigma_M(\mathbf{k} + \mathbf{q}, \epsilon_{\mathbf{k}+\mathbf{q}}/\hbar + \omega)$ in the construction of the RPA polarizability.

Generally, the inclusion of dynamical self-energy effects is expected to influence single-particle states by (i) renormalizing their energy due to the interaction with phonons; (ii) introducing an imaginary energy component that reflects the emergence of finite lifetime effects; (iii) leading to non-trivial dynamical (frequency-dependent) structures in the spectral function. In the context of photoemission spectroscopy, the aspects (i-iii) have been thoroughly characterized via first-principles calculations and experiments, and they are known to underpin the formation of photoemission kinks,² the emergence of polaronic satellites close to the band edges,³⁻⁵ as

well as the temperature-dependence of the band gap of insulators and semiconductors.^{7,10} In the following, we compute the dielectric function in the Fan-Migdal approximation to investigate the influence of (i-iii) on plasmons and electron-hole excitations.

In the clumped-nuclei approximation, whereby electron-phonon coupling is ignored, the inclusion of dynamical effects through the GW self-energy in the evaluation of the dielectric function may result in an unphysical renormalization of the intensity of calculated optical spectra if vertex corrections are neglected.⁵² For the case in which only the electron-electron interaction is treated, vertex corrections compensate the dynamical self-energy effects and are important to achieve good agreement with experiments.^{53,54} In the case of electron-phonon coupling, on the other hand, Migdal's theorem establishes that vertex corrections scale as $(m/M)^{1/2}$, where m and M are the electronic and ionic masses, respectively, suggesting that compensation effects due to the vertex should not alter the optical properties significantly.⁴² However, the importance of vertex corrections for electron-phonon interaction remains an open question that calls for further investigations.

III. PLASMON-PHONON COUPLING IN THREE DIMENSIONS

We account for the effects of electron-phonon interaction in the dielectric function through the numerical solution of Eqs. (1)-(5). We consider first a three-dimensional (3D) homogeneous electron gas with energy-momentum dispersion relations $\epsilon_{\mathbf{k}} = \frac{\hbar^2 k^2}{2m^*}$, where m^* is the effective mass. In the following we set $m^* = 0.2m_e$, a representative value for describing carriers at the band edges of doped semiconductors. The dielectric function in Eq. (1) is evaluated using the 3D Fourier transform of the bare Coulomb interaction: $v(\mathbf{q}) = 4\pi e^2/\epsilon_0 \mathbf{q}^2$, where ϵ_0 is the vacuum permittivity. In absence of electron-phonon interaction, the polarizability may be expressed analytically by the Lindhard function.^{55,56} Conversely, in presence of electron-phonon coupling, the momentum integral in Eq. (5) needs to be carried out numerically even for the HEG. The Fan-Migdal self-energy in Eq. (4) is evaluated by considering coupling to a single non-dispersive optical phonon mode (Einstein model) with energy $\hbar\omega_{\text{ph}} = 100$ meV, and an average electron-phonon coupling matrix element $\bar{g} = \langle g_{\mathbf{k}\mathbf{q}}^{\nu} \rangle = 100$ meV. This value is representative of materials characterized by strong coupling to LO phonons such as, for instance, TiO_2 ⁵⁷, EuO ⁶, and SrTiO_3 ⁴. We consider the Wigner-Seitz radii $r_s = 4$ and 16 , which correspond to carrier densities of $2.5 \cdot 10^{22}$ and $4 \cdot 10^{20}$ cm^{-3} , respectively, which are representative of metals and heavily-doped semiconductors. To quantify the effects of the electron-phonon interaction on the dielectric function and on the plasmon dispersion, we inspect in the following the loss function $L(\mathbf{q}, \omega) = \text{Im}[\epsilon^{-1}(\mathbf{q}, \omega)]$, which has poles at the energies

and momenta resonant with the excitation of plasmons and electron-hole pairs.⁵⁸ An introduction to the general features of the loss function for the 3D HEG can be found elsewhere.³³

In Fig. 2, we compare the RPA loss function of the 3D HEG with the case of the coupled electron-phonon system. In presence of electron-phonon interaction, $L(\mathbf{q}, \omega)$ exhibits qualitatively similar features to the RPA: there exists a critical momentum cutoff q_c^L such that (i) a sharp plasmon peak is visible at momenta $q < q_c^L$ whereas (ii) for larger momenta, $q > q_c^L$, the plasmon energy and momentum become degenerate with those of electron-hole excitations. The momentum cutoff can be expressed as³³ $q_c^L = k_F [(1 + \hbar\omega_{pl}/\epsilon_F)^{1/2} - 1]$, and its values for $r_s = 4$ and 16 are marked in Fig. 2 by dashed blue lines, where k_F and ϵ_F are the Fermi wavevector and the Fermi energy, respectively. $\hbar\omega_{pl} = \hbar(4\pi e^2 n / \epsilon_0 m^*)^{1/2}$ is the plasmon energy, which depends on the carrier concentration n and amounts to 1.2 eV (0.15 eV) for $r_s = 4$ ($r_s = 16$). While for $q > q_c^L$ plasmons decay primarily through the excitation of electron-hole pairs (Landau damping), for $q < q_c^L$ phonons constitute the principal plasmon-damping mechanism. In this region, the electron-phonon interaction induces a broadening of the plasmon peaks, reflecting finite lifetime effects due to the possibility of plasmon damping upon phonon emission. For both values of r_s , the characteristic energy scales of plasmon and electron-hole excitations are larger than the phonon energy, and phonon-induced damping induces a structureless homogeneous broadening of the loss function. The full width at half maximum of the plasmon peak, induced by the coupling to phonons, amounts to 20 and 5 meV for $r_s = 4$ and 16, respectively.

A quantitative estimation of the effects of phonons on the characteristic timescales of plasmon damping, is provided by the plasmon lifetime, which can be expressed as:⁵⁵

$$\tau_{\mathbf{q}} = \hbar^{-1} \left[\frac{\text{Im} P(\mathbf{q}, \omega_{\mathbf{q}}^{pl})}{[\partial \text{Re} P(\mathbf{q}, \omega) / \partial \omega]_{\omega = \omega_{\mathbf{q}}^{pl}}} \right]^{-1}. \quad (6)$$

Through the evaluation of Eq. (6), we obtain an average lifetime of 130 fs (750 fs) for $r_s = 4$ ($r_s = 16$) for momenta $q < q_c^L$. The plasmon lifetime drops rapidly to values $\tau_{\mathbf{q}} < 1$ fs for $q > q_c^L$ owing to the effectiveness of the electron-hole scattering mechanism.

If the coupling to phonons is neglected, electron-hole scattering is the sole decay pathway that plasmons may undergo. Correspondingly, the plasmon linewidth is infinitesimal for $q < q_c^L$, and the lifetime infinite. The broadening of the plasmon peak in Fig. 2 (a)-(b) stems from the imaginary component added to the denominator of RPA polarizability and necessary to converge the momentum integrals,⁵⁹ which amount to 5 and 1 meV for $r_s = 4$ and 16, respectively.

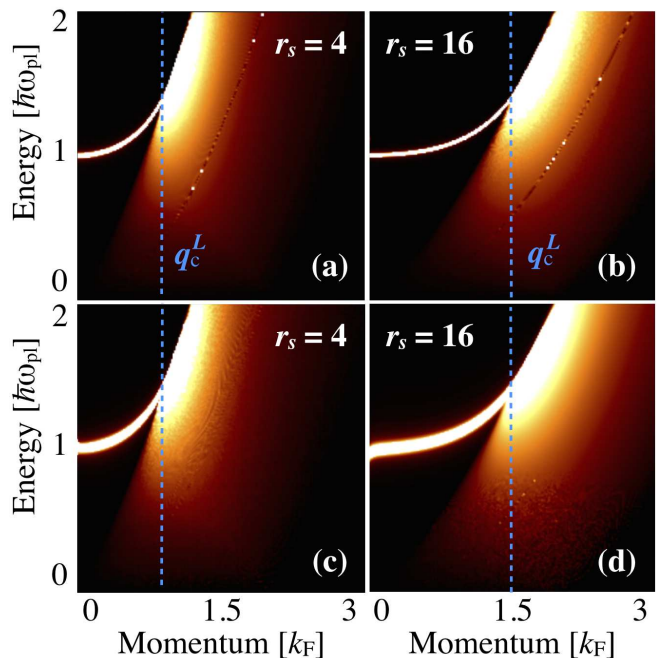


Figure 2. Loss function of the 3D HEG in the RPA (a)-(b) and for the coupled electron-phonon system (c)-(d) for $r_s = 4$ and 16. The critical momentum q_c^L (vertical dashed line) marks the onset of Landau damping. Energy is in units of the plasma energy ($\hbar\omega = 1.2$ and 0.15 eV for $r_s = 4$ and 16, respectively), whereas momentum is expressed in terms of the Fermi momentum ($k_F = 0.18$ and 0.045 \AA^{-1} for $r_s = 4$ and 16, respectively).

IV. PLASMON-PHONON COUPLING IN TWO DIMENSIONS

We now proceed to discuss general features of plasmon-phonon interaction in the 2D HEG. We consider again $r_s = 4$ and 16, which in 2D correspond to carrier concentrations of $5 \cdot 10^{15}$ and $1.2 \cdot 10^{15} \text{ cm}^{-2}$, respectively. The dielectric function is evaluated considering the 2D Fourier transform of the Coulomb interaction $v(\mathbf{q}) = 2\pi e^2 / \mathbf{q}\epsilon_0$. The loss function evaluated in absence of coupling to phonons is reported in Fig. 3 (a)-(b), where energies are in units of the plasma energy of the 3D HEG. The lower dimensionality has a striking effect on the energy dispersion of plasmons which, in 2D, is proportional to \sqrt{q} in the long-wavelength limit.⁵⁶ Similarly to the 3D case, there exists a critical momentum q_c^L such that 2D plasmons are undamped for $q < q_c^L$, whereas for $q > q_c^L$ they undergo Landau damping and decay upon excitation of electron-hole pairs.

When the electron-phonon interaction is switched on, the loss function of the 2D HEG, illustrated in Fig. 3 (c)-(d), reveals the emergence of more complex features as compared to the 3D case. For plasmon energies smaller than the phonon energy ($\hbar\omega_{pl} < \hbar\omega_{ph}$) the coupling between plasmons and phonons is forbidden by energy conservation, and the loss function resembles the case in

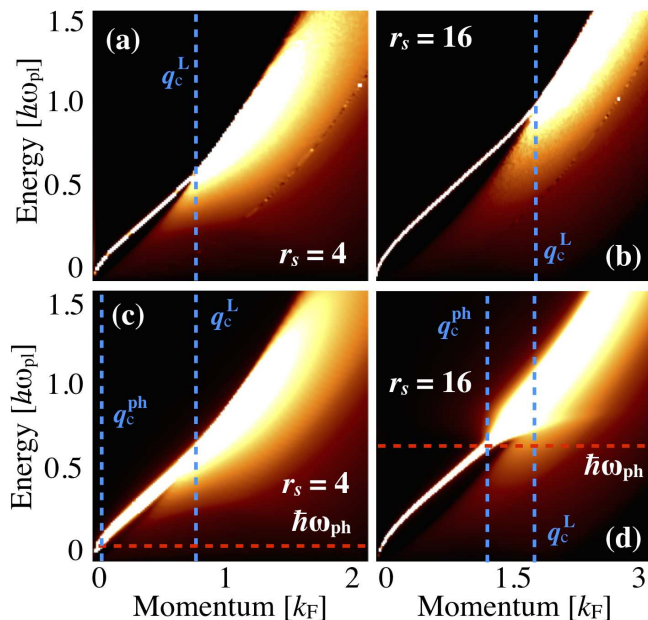


Figure 3. Loss function of the 2D HEG in the RPA (a)-(b) and for the coupled electron-phonon system (c)-(d) for $r_s = 4$ and 16. The critical momenta q_c^{ph} and q_c^{L} , shown as vertical dashed lines, mark the onset of phonon and Landau damping, respectively. Energy is in units of the plasma energy of the 3D HEG (*cf.* caption of Fig. 2).

which electron-phonon coupling is neglected. Conversely, for $\hbar\omega_{\text{pl}} > \hbar\omega_{\text{ph}}$ the effects of electron-phonon coupling on the plasmon dispersions is two-fold: (i) the plasmon peak is broadened by finite lifetime effects, (ii) the plasmon energy is renormalized and the corresponding peak is broadened. The combination of (i) and (ii) leads to the formation of a *kink* in the plasmon dispersion of 2D metals, in close analogy to the kink induced in the photoemission spectrum of solids by electron-phonon interaction.²

In addition to the critical momentum q_c^{L} for the onset of Landau damping, the coupling to optical phonons, thus, introduces a second critical momentum q_c^{ph} , defined by the condition $\omega^{\text{pl}}(q_c^{\text{ph}}) = \omega_{\text{ph}}(q_c^{\text{ph}})$, which marks the onset of plasmon decay upon phonon emission. An approximate explicit expression for q_c^{ph} can be obtained by approximating the plasmon dispersion by $\omega_{\mathbf{q}}^{\text{pl}} = (2\pi n e^2 q / m^* \epsilon_0)^{\frac{1}{2}}$, yielding $q_c^{\text{ph}} = \omega_{\text{ph}}^2 m^* \epsilon_0 / 2\pi n e^2$.

The values of q_c^{ph} and q_c^{L} are illustrated in Fig. 3 (c)-(d) as vertical dashed lines. In summary, for $q < q_c^{\text{ph}}$ plasmons are undamped; for $q_c^{\text{ph}} < q < q_c^{\text{L}}$, plasmons may decay upon scattering with phonons; for $q > q_c^{\text{L}}$, both phonons and Landau damping contribute to plasmon dissipation. While the coupling to acoustic phonons and electron-electron interaction are neglected here, in real solids these mechanisms are expected to provide additional dissipation channels that may lead to plasmon damping also in the limit $\mathbf{q} \rightarrow 0$, and they might thus constitute the primary decay mechanism for the long-wavelength plasmons in 2D.^{60,61}

Finally, we note that, despite the dependence of the numerical results of Figs. 2 and 3 on the model parameters \bar{g} and $\hbar\omega_{\text{E}}$, this qualitative picture is expected to hold also for parameter values different from those considered above. In particular, a decrease in the value of the effective electron-phonon coupling strength \bar{g} has the effect of reducing the overall influence of electron-phonon interaction on the loss function through a decrease in the broadening of the plasmon peaks. In the limit of vanishing coupling strength $\bar{g} \rightarrow 0$, the RPA results are recovered. While the precise value of the phonon energy $\hbar\omega_{\text{E}}$ does not affect significantly the loss function in 3D metals, in the 2D case $\hbar\omega_{\text{E}}$ defines the energy onset for the scattering between electrons and phonons, marked by horizontal dashed lines in Fig. 3 (c)-(d). Therefore, different values of the optical phonon energy are expected to alter the energy window in which the plasmon dispersion is broadened by lifetime effects.

V. APPROXIMATE TREATMENT OF ELECTRON-PHONON INTERACTION

First-principles calculations of the polarization in the Fan-Migdal approximation based on the solution of Eq. (5) may be possible for simple solids, however, the computational cost entailed by the evaluation of the electron-hole self-energy $\Delta\Sigma(\mathbf{k}, \mathbf{q}, \omega, \epsilon_{\mathbf{k}}/\hbar)$ may obstruct the application to systems with more than a few atoms per unit cell. To account for the effects of electron-phonon interaction in the loss function of crystalline solids, it is thus desirable to circumvent the computation of the electron-hole self-energy through approximations capable of reproducing the main features of the loss function at a reduced computational cost. We follow the approach introduced by Allen⁶² and subsequently generalized to first-principles calculations in Ref. 26, whereby $\Delta\Sigma(\mathbf{k}, \mathbf{q}, \omega, \epsilon_{\mathbf{k}}/\hbar)$ is approximated by its average over the Fermi surface in the optical limit ($\mathbf{q} \rightarrow 0$). Within these approximations, the polarization can be expressed as:^{62,63}

$$P(\mathbf{q}, \omega) = 2 \sum_{\mathbf{k}} \frac{f_{\mathbf{k}} - f_{\mathbf{k}+\mathbf{q}}}{\hbar\omega[1 + \lambda(\omega)] + i/\tau(\omega) + \epsilon_{\mathbf{k}} - \epsilon_{\mathbf{k}+\mathbf{q}}} \quad (7)$$

where we introduced the dynamical renormalization λ and the scattering time τ functions:

$$\tau^{-1}(\omega) = \frac{2\pi\hbar}{\omega} \int_0^{\omega} d\omega' (\omega - \omega') \alpha^2 F(\omega') \quad (8)$$

$$\lambda(\omega) = -\frac{2}{\omega} \int_0^{\infty} d\omega' \alpha^2 F(\omega') \times \left[\ln \left| \frac{\omega - \omega'}{\omega + \omega'} \right| - \frac{\omega'}{\omega} \ln \left| \frac{\omega^2 - \omega'^2}{\omega'^2} \right| \right] \quad (9)$$

$\alpha^2 F$ is the Eliashberg spectral function and it is defined as:

$$\alpha^2 F(\omega) = \frac{1}{2} \sum_{\mathbf{q}\nu} \omega_{\mathbf{q}\nu} \lambda_{\mathbf{q}\nu} \delta(\omega - \omega_{\mathbf{q}\nu}), \quad (10)$$

where the sum extends over all phonon modes ν and momenta \mathbf{q} . The electron-phonon coupling strength is given by:

$$\lambda_{\mathbf{q}\nu} = \frac{1}{N_F \omega_{\mathbf{q}\nu}} \sum_{\mathbf{k}} |g^\nu(\mathbf{k}, \mathbf{q})|^2 \delta(\epsilon_{\mathbf{k}} - \epsilon_F) \delta(\epsilon_{\mathbf{k}+\mathbf{q}} - \epsilon_F),$$

with N_F being the density of states at the Fermi energy. If we consider an Einstein model for the phonon dispersion with energy $\hbar\omega_{\text{ph}}$ and isotropic electron-phonon matrix elements \bar{g} , the electron-phonon coupling strength and the Eliashberg spectral function simplify to $\lambda_{\mathbf{q}} = \bar{g}^2/\omega_{\text{ph}}$ and $\alpha^2 F(\omega) = \bar{g}^2 \delta(\omega - \omega_{\text{ph}})/2$. Correspondingly, τ and λ can be evaluated analytically from Eqs. (8) and (9), and yield:

$$\tau_E^{-1}(\omega) = \bar{g}^2 \pi \hbar \frac{\omega - \omega_{\text{ph}}}{\omega} \theta(\omega - \omega_{\text{ph}}).$$

$$\lambda_E(\omega) = -\frac{\bar{g}^2}{\omega} \left[\ln \left| \frac{\omega - \omega_{\text{ph}}}{\omega + \omega_{\text{ph}}} \right| - \frac{\omega_{\text{ph}}}{\omega} \ln \left| \frac{\omega^2 - \omega_{\text{ph}}^2}{\omega_{\text{ph}}^2} \right| \right].$$

The resulting scattering rate τ_E and dynamical renormalization λ_E for the Einstein model are shown in Fig. 4 (a). τ_E^{-1} vanishes for $\omega < \omega_{\text{ph}}$, and it reflects the fact that the transfer of the plasmon energy to a phonon is forbidden by energy conservation and, correspondingly, no damping due to phonons may take place for frequency smaller than the phonon frequency. At large frequencies $\omega \gg \omega_{\text{ph}}$, the damping function saturates at the value $\tau_\infty^{-1} = \bar{g}^2 \pi$. These observations are consistent with the results of the 3D HEG, shown in Fig. 3, where the coupling to phonons induces a quasi-homogeneous broadening of the loss function for $\hbar\omega \gg \omega_{\text{ph}}$. The loss function obtained by combining Eq. (7) with the Einstein model for the scattering time and dynamical renormalization is exemplified in Fig. 4 (b) for $r_s = 16$. The model correctly reproduces the emergence of plasmon damping for $q > q_c^{\text{ph}}$, and the resulting formation of a kink in the plasmon dispersion. Despite the simplicity of the Einstein model, the trend of τ_E and λ_E is in good qualitative agreement with the result of first-principles calculations of Ref. 26.

Overall, these results suggest that the treatment of electron-phonon coupling through the effective dynamical-renormalization and scattering-time functions suffices to reproduce the main features obtained from the solution of the Hedin-Baym equations in the Fan-Migdal approximation, thus, validating earlier approximations for the optical conductivity,⁶² as well as recent first-principles calculations for doped graphene.²⁶ Additionally, a simplified approach based on the Einstein model may also provide a suitable framework to account for electron-phonon coupling in first-principles calculations

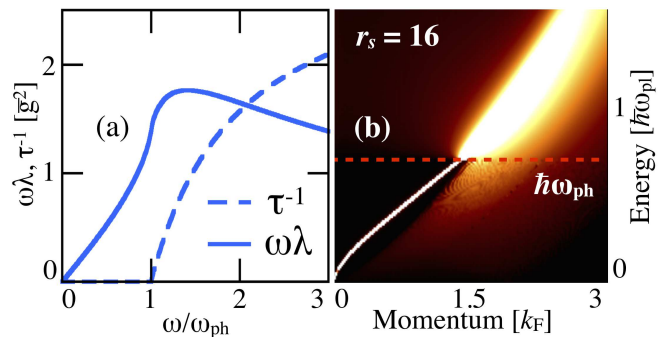


Figure 4. (a) Dynamical renormalization λ and scattering time τ^{-1} for the Einstein model. (b) Loss function of the 2D HEG for $r_s = 16$ obtained from Eq. (7) using λ and τ^{-1} illustrated in panels (a).

of the dielectric properties at a reduced computational cost. For instance, the ω_{ph} , and \bar{g} can be extracted from first-principles calculations, and Eq. (7) obtained using single-particle energies and oscillator strengths based on density-functional theory.

VI. CONCLUSIONS

We have investigated the influence of the electron-phonon interaction on the dissipation of plasmons in metals based on the solution of the Hedin-Baym equations for the dielectric function in the Fan-Migdal approximation. We have reported calculations of the loss function of the HEG in 2D and 3D and discussed the general features induced by electron-phonon coupling in the plasmon dispersion for carrier densities representative of metals and heavily-doped semiconductors. The coupling to phonons in 3D leads primarily to a broadening of the plasmon peak and to finite-lifetime effects. In addition to these signatures of plasmon-phonon coupling, our loss-function calculation for 2D systems also indicate the emergence of a kink in the plasmon dispersion – in close analogy to the kinks in photoemission spectroscopy – which arises from the coupling to a longitudinal optical phonon mode. In conclusion, these results call for further work to investigate compensation effects arising from the inclusion of vertex corrections,⁵³ the interplay of the electron-electron and electron-phonon interaction on the plasmon dispersion, as well as the temperature dependence of plasmon damping.

ACKNOWLEDGMENTS

Discussions with Pierluigi Cudazzo and Lucia Reining are gratefully acknowledged. FC and CD gratefully acknowledge financial support from the German Science Foundation (DFG) through the Collaborative Research Center HIOS (SFB 951).

- ¹ F. Giustino, *Rev. Mod. Phys.* **89**, 015003 (2017).
- ² A. Damascelli, Z. Hussain, and Z.-X. Shen, *Rev. Mod. Phys.* **75**, 473 (2003).
- ³ S. Moser, L. Moreschini, J. Jaćimović, O. S. Barišić, H. Berger, A. Magrez, Y. J. Chang, K. S. Kim, A. Bostwick, E. Rotenberg, L. Forró, and M. Grioni, *Phys. Rev. Lett.* **110**, 196403 (2013).
- ⁴ Z. Wang, S. McKeown Walker, A. Tamai, Y. Wang, Z. Ristic, F. Y. Bruno, A. de la Torre, S. Riccò, N. C. Plumb, M. Shi, P. Hlawenka, J. Sánchez-Barriga, A. Varykhalov, T. K. Kim, M. Hoesch, P. D. C. King, W. Meevasana, U. Diebold, J. Mesot, B. Moritz, T. P. Devereaux, M. Radovic, and F. Baumberger, *Nat. Mater.* **15**, 835 (2016).
- ⁵ C. Verdi, F. Caruso, and F. Giustino, *Nat. Commun.* **8**, 15769 (2017).
- ⁶ J. M. Riley, F. Caruso, C. Verdi, L. B. Duffy, M. D. Watson, L. Bawden, K. Volckaert, G. van der Laan, T. Hesjedal, M. Hoesch, F. Giustino, and P. D. C. King, Submitted (2017).
- ⁷ S. Logothetidis, J. Petalas, H. M. Polatoglou, and D. Fuchs, *Phys. Rev. B* **46**, 4483 (1992).
- ⁸ A. Eiguren and C. Ambrosch-Draxl, *Phys. Rev. Lett.* **101**, 036402 (2008).
- ⁹ A. Eiguren, C. Ambrosch-Draxl, and P. M. Echenique, *Phys. Rev. B* **79**, 245103 (2009).
- ¹⁰ F. Giustino, S. G. Louie, and M. L. Cohen, *Phys. Rev. Lett.* **105**, 265501 (2010).
- ¹¹ S. Poncé, G. Antonius, Y. Gillet, P. Boulanger, J. Laflamme Janssen, A. Marini, M. Côté, and X. Gonze, *Phys. Rev. B* **90**, 214304 (2014).
- ¹² G. Antonius, S. Poncé, P. Boulanger, M. Côté, and X. Gonze, *Phys. Rev. Lett.* **112**, 215501 (2014).
- ¹³ G. E. Jellison and F. A. Modine, *Phys. Rev. B* **27**, 7466 (1983).
- ¹⁴ P. Lautenschlager, M. Garriga, L. Vina, and M. Cardona, *Phys. Rev. B* **36**, 4821 (1987).
- ¹⁵ A. Marini, *Phys. Rev. Lett.* **101**, 106405 (2008).
- ¹⁶ W. Kohn, *Phys. Rev. Lett.* **2**, 393 (1959).
- ¹⁷ S. Piscanec, M. Lazzeri, F. Mauri, A. C. Ferrari, and J. Robertson, *Phys. Rev. Lett.* **93**, 185503 (2004).
- ¹⁸ M. Lazzeri and F. Mauri, *Phys. Rev. Lett.* **97**, 266407 (2006).
- ¹⁹ F. Caruso, M. Hoesch, P. Achatz, J. Serrano, M. Krisch, E. Bustarret, and F. Giustino, *Phys. Rev. Lett.* **119**, 017001 (2017).
- ²⁰ J. Schrieffer, *Theory Of Superconductivity* (Avalon Publishing, 1983).
- ²¹ M. Bernardi, D. Vigil-Fowler, J. Lischner, J. B. Neaton, and S. G. Louie, *Phys. Rev. Lett.* **112**, 257402 (2014).
- ²² M. Bernardi, D. Vigil-Fowler, C. S. Ong, J. B. Neaton, and S. G. Louie, *Proc. Natl. Acad. Sc.* **112**, 5291 (2015).
- ²³ F. Caruso and F. Giustino, *Phys. Rev. B* **94**, 115208 (2016).
- ²⁴ M. Bernardi, J. Mustafa, J. B. Neaton, and S. G. Louie, *Nature Comm.* **6**, 7044 (2015).
- ²⁵ A. M. Brown, R. Sundararaman, P. Narang, W. A. Goddard, and H. A. Atwater, *ACS Nano* **10**, 957 (2016).
- ²⁶ D. Novko, *Nano Lett.* **17**, 6991 (2017).
- ²⁷ G. Grimvall, *The electron-phonon interaction in metals* (North-Holland Pub. Co., 1981).
- ²⁸ M. W. Knight, H. Sobhani, P. Nordlander, and N. J. Halas, *Science* **332**, 702 (2011).
- ²⁹ L. R. Hirsch *et al.*, *Proc. Nat. Ac. Sc.* **23**, 100 (2003).
- ³⁰ D. O'Neal, L. R. Hirsch, N. J. Halas, J. Payne, and J. L. West, *Cancer Lett.* **209**, 171 (2004).
- ³¹ M. L. Brongersma, N. J. Halas, and P. Nordlander, *Nat. Nanotech.* **10**, 25 (2015).
- ³² J. B. Khurgin, *Nat. Nanotech.* **10**, 2 (2015).
- ³³ D. Pines, *Elementary Excitations in Solids* (Perseus, 1999).
- ³⁴ T. Holstein, *Ann. Phys.* **29**, 410 (1964).
- ³⁵ J. Noffsinger, E. Kioupakis, C. G. Van de Walle, S. G. Louie, and M. L. Cohen, *Phys. Rev. Lett.* **108**, 167402 (2012).
- ³⁶ C. E. Patrick and F. Giustino, *J. Phys.: Condens. Matter* **26**, 365503 (2014).
- ³⁷ M. Zacharias, C. E. Patrick, and F. Giustino, *Phys. Rev. Lett.* **115**, 177401 (2015).
- ³⁸ M. Zacharias and F. Giustino, *Phys. Rev. B* **94**, 075125 (2016).
- ³⁹ A. Molina-Sánchez, M. Palummo, A. Marini, and L. Wirtz, *Phys. Rev. B* **93**, 155435 (2016).
- ⁴⁰ G. Antonius and S. G. Louie, (2017), arXiv:1705.04245.
- ⁴¹ L. Hedin and S. Lundqvist, *Solid State Physics*, **23**, 1 (1970).
- ⁴² M. A. Sov. Phys. JETP **7**, 996 (1958).
- ⁴³ A. Lanzara, P. Bogdanov, X. Zhou, S. Kellar, D. Feng, E. Lu, T. Yoshida, H. Eisaki, A. Fujimori, K. Kishio, J. Shimoyama, T. Noda, S. Uchida, Z. Hussain, and Z. Shen, *Nature* **412**, 510 (2001).
- ⁴⁴ A. Bostwick, T. Ohta, T. Seyller, K. Horn, and E. Rotenberg, *Nature Phys.* , 36 (2007).
- ⁴⁵ F. Mazzola, J. W. Wells, R. Yakimova, S. Ulstrup, J. A. Miwa, R. Balog, M. Bianchi, M. Leandersson, J. Adell, P. Hofmann, and T. Balasubramanian, *Phys. Rev. Lett.* **111**, 216806 (2013).
- ⁴⁶ M. S. Hybertsen and S. G. Louie, *Phys. Rev. B* **34**, 5390 (1986).
- ⁴⁷ B. Holm and U. von Barth, *Phys. Rev. B* **57**, 2108 (1998).
- ⁴⁸ F. Caruso, P. Rinke, X. Ren, A. Rubio, and M. Scheffler, *Phys. Rev. B* **88**, 075105 (2013).
- ⁴⁹ F. Caruso, M. Dauth, M. J. van Setten, and P. Rinke, *J. Chem. Theory Comput.* **12**, 5076 (2016), pMID: 27631585.
- ⁵⁰ I. Kupčić, *Phys. Rev. B* **91**, 205428 (2015).
- ⁵¹ J. Hwang, J. P. F. LeBlanc, and J. P. Carbotte, *J. Phys.: Condens. Matter* **24**, 245601 (2012).
- ⁵² R. Del Sole and R. Girlanda, *Phys. Rev. B* **54**, 14376 (1996).
- ⁵³ F. Bechstedt, K. Tenelsen, B. Adolph, and R. Del Sole, *Phys. Rev. Lett.* **78**, 1528 (1997).
- ⁵⁴ A. Marini and R. Del Sole, *Phys. Rev. Lett.* **91**, 176402 (2003).
- ⁵⁵ G. Mahan, *Many-Particle Physics* (Springer, 2000).
- ⁵⁶ G. Giuliani and G. Vignale, *Quantum Theory of the Electron Liquid* (Cambridge University Press, 2005).
- ⁵⁷ C. Verdi and F. Giustino, *Phys. Rev. Lett.* **115**, 176401 (2015).
- ⁵⁸ P. Nozières and D. Pines, *Phys. Rev.* **113**, 1254 (1959).
- ⁵⁹ F. Caruso and F. Giustino, *Eur. Phys. J. B* **89**, 238 (2016).
- ⁶⁰ A. Principi, M. Carrega, M. B. Lundeberg, A. Woessner, F. H. L. Koppens, G. Vignale, and M. Polini, *Phys. Rev. B* **90**, 165408 (2014).

- ⁶¹ D. Neilson, L. Świerkowski, A. Sjölander, and J. Szymański, Phys. Rev. B **44**, 6291 (1991).
- ⁶² P. B. Allen, Phys. Rev. B **3**, 305 (1971).
- ⁶³ I. Kupčić, Phys. Rev. B **95**, 035403 (2017).